Impairing temozolomide resistance driven by glioma stem-like cells with adjuvant immunotherapy targeting O-acetyl GD2 ganglioside

Julien Fleurence[1]*, Meriem Bahri[1]*, Sophie Fougeray[1,2], Sébastien Faraj[1,3], Sarah Vermeulen[1], Emilie Pinault[4], Fanny Geraldo[1], Lisa Oliver[1], Joëlle Véziers[5,6,7], Pierre Marquet[8], Marion Rabé[1], Catherine Gratas[1,3], François Vallette[1,9], Claire Pecqueur[1], François Paris[1,9] and Stéphane Birklé [1,2]

[1]CRCINA, INSERM, Université d'Angers, Université de Nantes, Nantes, France

[2]Université de Nantes, UFR des Sciences Pharmaceutiques et Biologiques, Nantes, France

[3]Centre Hospitalier Universitaire de Nantes, Nantes, France

[4]Univ. Limoges, BISCEm Mass Spectrometry Platform, Limoges, France

[5]INSERM, UMRS 1229, RMeS "Regenerative Medicine and Skeleton", Team STEP "Skeletal Physiopathology and Joint Regenerative Medicine", Nantes, France

[6]SC3M platform, UMS INSERM 016/CNRS 3556, SFR François Bonamy, Nantes, France

[7]CHU Nantes, PHU 4 OTONN, Nantes, France

[8]INSERM, Univ. Limoges, CHU Limoges, IPPRITT, U1248, Limoges, France

[9]LaBCT, Institut de Cancérologie de l'Ouest-René Gauducheau, Saint-Herblain, France

Stem cell chemoresistance remains challenging the efficacy of the front-line temozolomide against glioblastoma. Novel therapies are urgently needed to fight those cells in order to control tumor relapse. Here, we report that anti-O-acetyl-GD2 adjuvant immunotherapy controls glioma stem-like cell-driven chemoresistance. Using patient-derived glioblastoma cells, we found that glioma stem-like cells overexpressed O-acetyl-GD2. As a result, monoclonal antibody 8B6 immunotherapy significantly increased temozolomide genotoxicity and tumor cell death *in vitro* by enhancing temozolomide tumor uptake. Furthermore, the combination therapy decreased the expression of the glioma stem-like cell markers CD133 and Nestin and compromised glioma stem-like cell self-renewal capabilities. When tested *in vivo*, adjuvant 8B6 immunotherapy prevented the extension of the temozolomide-resistant glioma stem-like cell pool within the tumor bulk *in vivo* and was more effective than the single agent therapies. This is the first report demonstrating that anti-O-acetyl-GD2 monoclonal antibody 8B6 targets

Cancer Therapy and Prevention

glioblastoma in a manner that control temozolomide-resistance driven by glioma stem-like cells. Together our results offer a proof of concept for using anti-O-acetyl GD2 reagents in glioblastoma to develop more efficient combination therapies for malignant gliomas.

What's new?

Glioblastoma multiforme (GBM) is a complex malignancy harboring differentiated tumor-bulk cells and self-renewing GBM stem-like cells (GSCs). Targeting both cell compartments is necessary to improve prognosis. Here, the authors characterize OAcGD2 ganglioside as a novel GSCs marker that sensitizes chemo-resistant GSCs to TMZ. The combination of anti-OAcGD2 monoclonal antibody 8B6 with TMZ results in increased temozolomide genotoxicity and tumor cell death *in vitro* by enhancing temozolomide tumor uptake. Furthermore, 8B6 works synergistically with TMZ to compromise GSCs self-renewal. The identification of OAcGD2 as a GSC-associated antigen offers a novel opportunity for optimizing TMZ chemotherapy in GBM patients to prevent recurrence.

Introduction

The 5-year survival for patients with glioblastoma (GBM), the most common primary malignant brain tumor in adults, is a dim 10%.[1] The current standard of care starts with maximal safe resection, followed by radiation therapy with chemotherapy and adjuvant chemotherapy.[2] The chemotherapeutic agent Temodar (temozolomide, TMZ) is currently used as part of this first-line treatment.[2] Its therapeutic benefit depends on its ability to methylate DNA, which results in the highest cytotoxicity when it occurs at the O^6 position of guanine.[3] The O^6-alkylguanine adducts initiate mismatch abortive repair and DNA fragmentation, thus causing cell cycle arrest and ultimately cell death.[3] Even with such multimodal treatment, the overall survival does not exceed 15–19 months, with a high-rate of tumor recurrence.[2] Consequently, there is a clear and urgent need for more effective initial therapy.

A major challenge in treating GBM is due to its inherent heterogeneity, both at the cellular and the molecular levels. Among the GBM cellular mass, it appears that a small subpopulation of self-renewing cells expressing specific markers, are considered responsible for tumor initiation, maintenance and recurrence.[4] These cells, named glioblastoma stem-like cells (GSCs),[5] are generally not completely removed by surgery and are resistant to chemotherapy and radiotherapy, allowing surviving GSCs to regenerate the tumor and promote recurrence.[6,7]

At the molecular level, drug resistance is conferred by various mechanisms. The most established cause of TMZ-resistance is associated with the upregulation of O^6-methylguanine–DNA methyltransferase (MGMT), an enzyme that repairs DNA damage induced by TMZ.[8] Molecular examination of GSCs revealed additional MGMT-independent resistance mechanisms including defective apoptotic regulation and enhanced prosurvival signaling.[9–11] These mechanisms, with the strong propensity for tumor formation, support adaptation to environmental stress and promote tumor recurrence.[8] Many targeted therapies have

been under clinical evaluation, and unfortunately, have not achieved significant extension of the patients' overall survival.[12] Since these therapies only target a single signaling pathway, it was proposed that they are not sufficient enough to inhibit GBM proliferation, which arises, as mentioned above, from many defective-signaling pathways.[13] This emphasizes the option for novel combination therapy strategies that effectively increase response of GBM tumor bulk cells and GSCs to TMZ therapy.

By proposing to target the GSC subset and the GBM tumor bulk, the identification of a specific marker shared by both cell populations is mandatory. Currently published antigens, such as EGFRvIII,[14] Her-2[15] or interleukin-13 receptor subunit alpha-2 (IL13Ra2),[16] represent non-homogeneously expressed antigens.[17] Targeting these antigens, therefore, cannot avoid relapse from the outgrowth of antigen null tumor cells.[18,19] Novel homogeneously expressed specific antigens within the tumor need to be characterized.

We have previously identified O-acetyl derivative of GD2 ganglioside, namely, O-acetyl-GD2 (OAcGD2), as a new target antigen for GBM immunotherapy with monoclonal antibodies (mAbs).[20] The mechanisms by which anti-OAcGD2 mAbs induce GBM tumor cell killing involve antibody-dependent cell cytotoxicity and induction of cell death[20] with features of oncosis.[21] Moreover, OAcGD2 expression prevails post immunotherapy *in vivo*, suggesting the absence of an immunoediting process that would select OAcGD2-negative tumor cells.[20] However, the expression of OAcGD2 on GSCs has not been investigated yet. Taking into account that (*i*) tumor-associated ganglioside antigens can be expressed by cancer stem-like cells[22] and (*ii*) the proapoptotic activity displayed by anti-OAcGD2 mAbs, we investigated here whether the OAcGD2 may serve as a chemosensitizing target in GSC. We find that OAcGD2 is expressed by GSCs and further show that the combination of anti-OAcGD2 mAbs strikingly works synergistically with TMZ to compromise GSCs self-renewal.

Materials and Methods

Pharmacological agents

Anti-OAcGD2 mAb 8B6 and anti-DOTA mAb IgG2a were obtained previously.[20,21] TMZ was purchased from Interchim (Montluçon, France). TMZ was reconstituted with dimethylsulfoxide (DMSO) as stock solution and aliquots were stored at −20°C. DMSO at a final percentage equivalent to that of the TMZ solution served as the vehicle control for all *in vitro* studies.

Cell lines and cell culture

Human GBM Hs683 (RRID:CVCL_844) and mouse neuroblastoma Neuro-2a (RRID:CVCL_0470) cell lines were obtained from ATCC (LGCstandard) and cultured in DMEM 4.5 g/l glucose containing 1% penicillin and streptomycin, supplemented with 10% fetal calf serum (FCS) and L-glutamine. GBM patient-derived cells were obtained as described previously.[20,23] Cells were maintained as neurospheres in DMEM/Ham F12 containing 1% penicillin and streptomycin supplemented with L-glutamine, B27, N2 supplement, and heparin (2 μg/ml), with additional growth factors β-FGF (40 ng/ml) and EGF (40 ng/ml) added extemporaneously. Culture reagents were obtained from Gibco Life Technologies (Waltham, MA). All cell types were kept at early passage and routinely tested for Mycoplasma by PCR. Hs683 cell line was authenticated using PCR-single-locus-technology analysis by Eurofins Genomics (Ebersberg, Germany). Patient-derived GBM cells were routinely tested by flow cytometry analysis for stem-like cell markers and self-renewal assay.

Flow cytometry binding analysis

O-Acetyl-GD2 expression analysis in GBM cells was performed by indirect immunofluorescence using flow cytometry (FCM). GBM neurospheres were dissociated with Accutase® solution (Sigma-Aldrich, St. Louis, MO). Hs683 cells were dissociated with trypsin–ethylenediaminetetraacetate (EDTA) solution (ThermoFisher Scientific, Illkirch, France). Cells in suspension were washed with phosphate-buffered saline (PBS), fixed with paraformaldehyde (PFA) 4% (Electron Microscopy Sciences, Hatfield, PA) for 10 min at 4°C, and then incubated with 8B6 (10 μg/ml) for 45 min. Antibody 8B6 binding was detected by incubation of a secondary, fluorescein isothiocyanate-labeled antibody (Jackson Immunoresearch, Soham, UK). For the quantification of OAcGD2 molecules, cellular antigen expression was measured as antibody binding capacity (ABC) units using the quantum Simply Cellular Kit (Bang Laboratories, Indianapolis, IN) per the manufacturer's instructions. The ABC values calculated for OAcGD2 after the subtraction of the values of the isotype control antibody were expressed as molecule per cell. Separate experiments were performed with the IgG control.

For stem cell marker expression analysis in GSCs, GBM were dissociated as described above and then permeabilized with saponin solution 0.5% (Sigma Aldrich, St. Louis, MO). Cells were then incubated with a PE-labeled anti-CD133/1 antibody (Clone AC133, Milltenyi, Bergisch Gladbach, Germany), or a V450-labeled anti-Nestin antibody (Clone 25, BD biosciences, Franklin Lakes, NJ), or an Alexa-Fluor 647 anti-Sox2 antibody (Clone 245610, BD bioscience) in the presence of 8B6, as described above. Separate experiments were performed with appropriate isotype-control antibodies. In both set of experiments, cell fluorescence was analyzed using a FACS Canto flow cytometer (BD Biosciences, San Jose, CA) and the FlowJo software (Flowjo LLC, Oregon, OR). For multiple test samples comparison between groups, a mean fluorescence intensity (MFI) ratio was calculated by dividing the flow cytometric MFI value of treated cells incubated with 8B6 and/or TMZ by the MFI value for the same cells left untreated. In some experiments, results were expressed as fold increase of the MFI ratio of the nontreated cells.

MGMT RNA expression assay

Cells were collected and RNA extracted using Nucleospin RNA/Protein kit (Macherey Nagel, Düren, Germany) according to the recommendations. DNAse treatment was included in the protocol. RNA concentration was evaluated using Nano-Drop® ND-1000 spectrophotometer (Nanodrop Technologies, Wilmington, DE) and RNA quality using the Agilent 2100 Bio-analyser (Agilent, Santa Clara, CA). All RNA integrity number (RIN) were >9. RNA reverse transcription was next performed using Maxima First Strand cDNA Synthesis Kit (Thermo Scientific, Waltham, MA). MGMT expression was then quantified by qPCR assay performed in triplicates using the real-time thermal cycler qTower (Analytik Jena AG, Germany). The Perfecta™ SYBR® Green FastMix™, Low ROX™ (Quanta BioSciences, Gaithersburg, MD) was used as recommended. Transcript expression was normalized to the mean of housekeeping genes (RPLPO, TATA, S28 and HGPRT) and expressed as follow: $(1/Ct\ normalized) \times 100$.

Cell viability analysis

We measured the cell viability using the MTT assay.[24] Cells (10^3–10^4) were seeded into a 96-well plate in 100 μl of media. The next day, 50 μl (three times concentrated) of several TMZ and/or 8B6 concentrations prepared in 1:2 serial dilutions were added for 72 hr. The day of the analysis, cells were incubated with MTT (Sigma-Aldrich) in culture medium for 4 hr. Formazan crystals were next dissolved in 100 μl of lysing solution (Sigma Aldrich). Absorbance values were recorded at 570 nm on a Multiskan reader (Thermo Electron). Assays were performed in quadruplicate and experiments were repeated three times. Percentage survival for each dose was calculated by multiplying absorbance values with 100 and divided by control absorbance value. Dose–response curves were analyzed using CompuSyn software (ComboSyn, Inc, Paranus, NJ) to determine the effective dose 50 (ED_{50}), 75 (ED_{75}) and 90 (ED_{90}) values.

Cancer Therapy and Prevention

Determination of synergy

Temozolomide and 8B6 interactions were analyzed for synergistic, additive or antagonistic effect using the combination index (CI) method developed by Chou and Talalay[25] as previously described.[26] The ED_{50} for TMZ and mAb was determined prior to experiment set up, as described above. The ED_{50} for 8B6 was reported previously.[20] Equipotent ratios of the two compounds were prepared across wide range of concentration. The cells were treated in 96-well plate for 72 hr. Percentage survival values obtained by MTT assay were converted into Fa (Fraction affected) values using the formula $1 - (\% \text{ survival}/100)$. These values were fed into CompuSyn software (ComboSyn, Inc, Paranus, NJ) to determine combination index values (CI = 1, additivity; CI > 1, antagonism; CI < 1, synergism) at ED_{50}, ED_{75} and ED_{90}. The mean CI value for each condition was determined by averaging the CI values of three independent experiments.

Limiting dilution assay

GBM cells were seeded at an initial concentration of 2×10^3 cells/ml from which serial dilutions were performed into a 96-well plate. Cells were then treated with TMZ (50 µM) and/or 8B6 (40 µg/ml). Two weeks later, each well was scored for neurosphere formation and the frequency of GSCs was calculated with the ELDA software.[27]

Scanning electron microscopy

Tumor cells (10^6) were incubated in culture media containing 8B6 (40 µg/ml), control antibody (40 µg/ml), TMZ (50 µM), TMZ + 8B6, respectively, for 30 min at 37°C. Cells were then washed with PBS, and then fixed with 2% glutaraldehyde (Sigma Aldrich) in PBS (4°C, 1 hr). Thereafter, cells were washed with PBS and postfixed in 1% OsO_4 for 15 min (Sigma Aldrich). Then, cells were washed again with PBS, and dehydrated through a graded ethanol (VWR Prolabo). Cells were finally gold coated for 2 min before analysis by Scanning Electron Microscope (Merlin, Carl Zeiss, Germany). Images were stored as TIFF files with Adobe Photoshop (Adobe System Incorporated, San Jose, CA).

Intracellular uptake of temozolomide

GBM-10 cells were incubated with 50 µM TMZ with or without 8B6 (40 µg/ml) for 30 min at 37°C, washed three times with PBS, and then centrifuged to harvest the pellet. TMZ, 5-(3-methyltriazen-1-yl)imidazole-4-carboxamide (MTIC) and internal standards (I.S.)—TMZ-d3 and MTIC-d3—were obtained from Toronto Research Chemicals (Toronto, Canada). LC–MS grade acetonitrile (ACN, 450 µl, Sigma-Aldrich) was added on the cell pellets followed by internal standard solution (50 µl, 100 ng/ml TMZ-d3–50 ng/ml MTIC-d3). Cell pellets were dispersed by sonication, and then centrifuged at 7,000g for 10 min at 4°C. Calibration standards were prepared at the following concentration levels: TMZ, 37.5 ng, 100 ng and 200 ng; MITC, 0.75 ng, 2 ng and 4 ng. Calibration standards and quality controls were prepared by spiking blank cell pellets with an appropriate volume of each standard solution. A 5 µl aliquot of the supernatant was chromatographed via HPLC using Waters Atlantis® HILIC Silica 5 µm (2.1 × 150 mm) column and introduced via electrospray into 4000 QTRAP mass spectrometer (Sciex). The gradient mobile phase consisted of 5 mM ammonium acetate (Fisher Scientific) pH 5 (A) and 98% ACN/2% A (B). The gradient was maintained at 100% B for 2 min, decreased to 70% B in 3 min, then to 5% B over the next minute and returning to 100% B in the last 5 min. The control samples were used for determination of the precision and accuracy of the method, precision being calculated as the coefficient of variation (CV %) within a single run (intra-assay; $n = 5$) and between different assays (interassay; $n = 5$), and accuracy as the percentage of deviation between nominal and found concentration with the established calibration curves. TMZ uptake was represented by the pooled concentration values of TMZ and TMZ derived-metabolites.

Evaluation of DNA breaks and tumor cell apoptosis

Cells (10^5) were plated in 12-well plates and incubated during 24 hr and then treated for 72 hr at 37 °C with 8B6 (40 µg/ml), TMZ (50 µM) or by combination of the two. To assess cell death, cells were incubated with propidium iodide (10 µg/ml; Sigma-Aldrich) for 15 min. To evaluate DNA damage, cells were fixed with paraformaldehyde (PFA) 4% (Electron Microscopy Sciences) and then permeabilized with saponin solution 0.5% (Sigma-Aldrich) before being incubated with a primary antiphosphorylated histone H2AX antibody (clone 20E3, Cell Signaling, Inc., Beverly, MA). Next, the cells were washed with PBS and incubated with a secondary, Alexa-Fluor 488 antibody (Cell Signaling Technology Inc.). DNA damages and apoptotic cells were then identified by FACSCalibur flow cytometer (BD Biosciences) using the FlowJo software (Treestar, Ashland, OR). For DNA damage analysis, a MFI ratio was calculated by dividing the flow cytometric MFI value of treated cells incubated with 8B6 and/or TMZ by the MFI value for the same cells left untreated, and results were expressed as fold increase of the MFI ratio of the nontreated cells.

In vivo glioblastoma formation

Subcutaneous GBM-10-bearing mice were obtained by s.c. injection of 10^6 GBM-10 cells into the flank of 8-week-old nonobese diabetic/severe combined immune-deficient gamma (NSG) mice (Charles River Laboratories, Wilmington, MA). Tumors and mouse body weight were measured every 3–4 days. Tumor volume was calculated as $mm^3 = (\text{width}^2 \times \text{lenght}) \times 0.5$. Mice with engrafted tumors that reached 30 mm^3 in size were randomized ($n = 10$ per condition). Thereafter, the mice received i.v. injection of 8B6 (75 µg) twice a week for 2 weeks, with or without concomitant i.p. injection of TMZ (0.5 mg/kg). Control groups consisted of mice receiving injections of PBS. The event resulting in mouse euthanasia was disease progression, defined as the tumor volume reaching above 0.5 cm^3.

Harvested tumor samples were dissociated using the human tumor dissociation kit and the gentleMACS Dissociator (Miltenyi) according to the manufacturer's instructions. Tumor cell suspensions were used for FCM assays to detect OAcGD2 and GSCs, and for LDA to assess GSC self-renewal propensity and frequency, as described above.
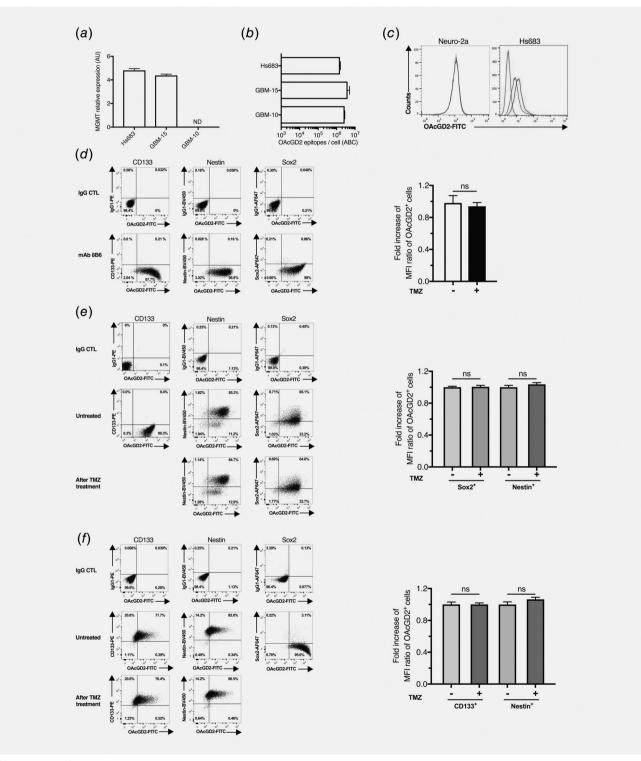

Figure 1. Legend on next page.

Cancer Therapy and Prevention

Statistics

Data are representative of three independent experiments run in triplicates, and expressed as mean ± standard error (SEM). For all *in vitro* experiment, *n* indicates the number of independent performed experiments. For all *in vivo* experiments, *n* indicates the number of animals we used. Comparison between groups *in vitro* and *in vivo* was performed using the Mann–Whitney test when possible (*n* > 3) and two-tailed unpaired Student's *t*-test (*n* = 3). All statistical analyses were performed using Prism software (v7.02, GraphPad Prism Software, La Jolla, CA). We considered a value $p < 0.05$ to be statistically significant.

Ethic statement

All GBM tissue collections and analysis were performed in accordance with the Institutional Review Board-approved protocol and all patients or their guardians provided written informed consent (*Comité de Protection des Personnes Ouest IV, protocol* # DC-2012-1555). All care of animals and experimental procedure were conducted under the approval of the French Government (Agreement APAFIS # 00186.02).

Data availability statement

Data can be provided upon request.

Results

Glioblastoma stem-like cells express O-acetyl GD2 ganglioside

Taking into account that almost half of GBMs are primarily resistant to TMZ, due to the expression of MGMT,[28] we first studied the MGMT-expression levels in GBM cells (Fig. 1b). Hs683 and GBM-15 cells express MGMT in contrast to GBM-10 cells (Fig. 1b). GBM-10 cells however express various genes that have been implicated in TMZ resistance such as Polymerase B, Notch, connexin 43, and NF-kB (Supporting Information Material S1).[9–11,29]

We have previously shown that GBM tumors express OAcGD2.[20] Figure 1b shows here that Hs683-, GBM-15- and GBM-10-cell populations express OAcGD2, with a calculated antibody binding capacity (ABC) of ∼1.5×10^6, ∼2.7×10^6 and ∼6×10^6 molecules/cell, respectively. We used the Neuro-2a cells as a negative control (Fig. 1c).[30]

One important obstacle against effective therapy is that GBMs is predominantly cause by self-renewing GSCs.[31,32] Thus, we questioned whether GSCs would express OAcGD2. We performed a FCM analysis using a combination of three relevant GSC markers (CD133, Sox 2 and Nestin) to identify any GSC-positive cell subsets.[33–35] We found that the Hs683 cell line does not contain any Nestin+-, CD133+- or Sox2+-GSC cell subsets (Fig. 1d). In contrast, GBM-10 or GBM-15 cells contain both GSC-negative and GSC-positive cell subsets (Figs. 2e and 2f). Notably, GBM-10 cells are composed of a Nestin+- and a CD133+-GSC subsets, but does not contain Sox2+-GSCs (Fig. 2e). In addition, GBM-15 cells contain both Nestin+- and Sox2+-GSCs, but no CD133+-GSC subset (Fig. 2f). Importantly, we found that all GSC-positive subsets express high level of OAcGD2 (Figs. 2e and 2f).

To build the rationale to combine TMZ with anti-OAcGD2 antibody, we next investigated whether TMZ would affect OAcGD2 expression on GBM cells, including on GSC-positive cell subsets. GBM-10 and GBM-15 cells were exposed for 72 hr to 50 μM TMZ, respectively, before FCM analysis. The duration of treatment was reported previously by others.[36] The selected TMZ concentration corresponds to the maximum plasma concentration achievable in patients at the therapeutic dosage.[37] The analysis of the MFI ratios indicates that OAcGD2 expression is unaltered after TMZ exposure in either the GSC-negative or the GSC-positive subsets (Figs. 1d-1f). These findings suggest that (*i*) it is possible to target both GSC-negative and GSC-positive subsets, (*ii*) anti-OAcGD2 mAbs represent adequate combination partners with TMZ.

Figure 1. Temozolomide exposure does not affect O-acetyl-GD2 (OAcGD2) expression in glioblastoma (GBM) cells. (*a*) Relative expression of MGMT in the indicated GBM cells assessed by qPCR, as described in the Materials and Methods section. ND, not detected. (*b*) Representative expression of OAcGD2 on Hs683, GBM-15 and GBM-10 cell surface, as indicated. Results are expressed as antibody binding capacity (ABC) molecules/cell. (*c*) OAcGD2 ganglioside expression level determined by FCM before and after exposition to 50 μM temozolomide (TMZ) for 72 hr. Representative FCM histograms of Neuro-2a, and Hs683, as indicated, stained with either control antibody (blue, untreated cells; orange, TMZ-treated cells) or 8B6 (purple, untreated cells; green, TMZ-treated cells). (*d*) Left Panels, representative dot-plot analysis showing the correlation of the expression CD133/OAcGD2, Nestin/OAcGD2 and Sox2/OAcGD2 in Hs683 cells before and after treatment with TMZ (50 μM, 72 hr), as indicated. Parallel samples were incubated with the isotype control antibody, as indicated. No expression of GSCs markers is observed. Right panel, surface OAcGD2 expression level in Hs683 cells before (empty column) and after TMZ (50 μM, black column) exposure (72 hr). Results are expressed as fold increase of the MFI ratio of the untreated cells, and are presented as mean ± SEM of three individual experiments, each run in triplicate. No significant change in surface OAcGD2 expression is seen after TMZ incubation (ns, not significant). (*e*) The same cytofluorimetric analysis was performed in GBM-15 cells. Left panels, representative dot-plot histograms showing the correlation of the expression CD133/OAcGD2, Nestin/OAcGD2 and Sox2/OAcGD2 in GBM-15 cells before and after treatments with TMZ, as indicated. Right panel, surface OAcGD2 expression level before and after TMZ incubation in either GSC-positive and GSC-negative cell subsets, as indicated. GBM-15 cell population contains a Sox2+- and a Nestin+-cell fractions. No significant change in surface OAcGD2 expression is seen after TMZ incubation in both cell subsets (ns, not significant). (*f*) The same cytofluorimetric analysis was performed with GBM-10 cells. GBM-10 cell population includes both a CD133+- and a Nestin+-cell subsets. No significant change in surface OAcGD2 expression is seen after TMZ incubation in both CD133+- and Nestin+-cell subsets (ns, not significant). No significant change in surface OAcGD2 expression is detected in both cell subsets ($p > 0.05$; Mann–Whitney test).
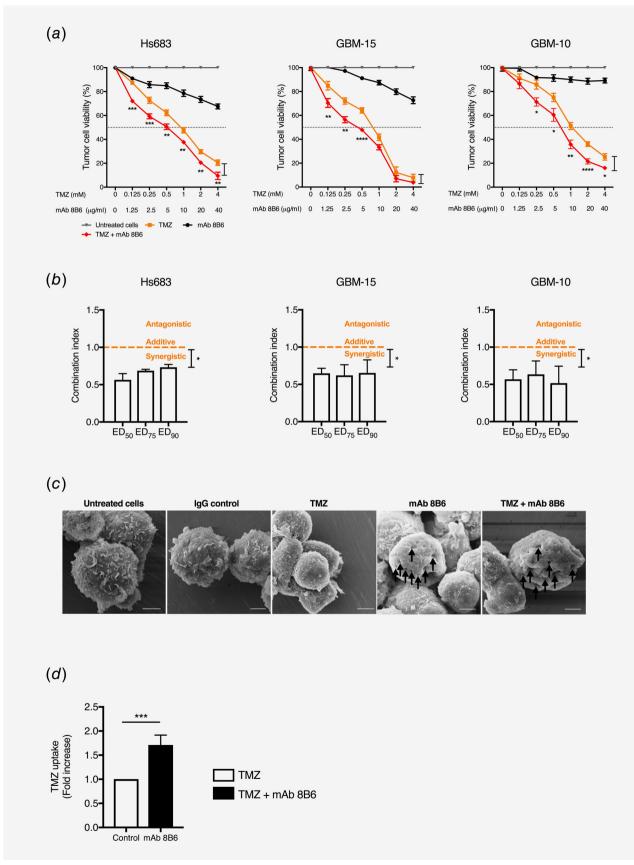
Figure 2. Legend on next page.

Table 1. Characterization of ED_{50}, ED_{75} and ED_{90} of temozolomide used as a single agent or in combination with 8B6

	ED^1 (μM)	TMZ alone	TMZ with mAb 8B6[2]	p value[3]	TMZ with IgG control[4]	p value[5]
Hs683	ED_{50}	1,079 ± 146	471 ± 24	‹0.01	1,049 ± 51	ns
	ED_{75}	3,468 ± 257	2,040 ± 226	‹0.01	3,476 ± 204	ns
	ED_{90}	12,170 ± 663	6,541 ± 868	‹0.01	11,516 ± 476	ns
GBM-15	ED_{50}	564 ± 77	330 ± 40	‹0.01	691 ± 113	ns
	ED_{75}	894 ± 94	640 ± 60	‹0.01	1,286 ± 333	ns
	ED_{90}	1,467 ± 66	1,167 ± 98	‹0.01	1,482 ± 38	ns
GBM-10	ED_{50}	1,313 ± 163	764 ± 191	‹0.01	1,662 ± 105	ns
	ED_{75}	5,255 ± 432	2,897 ± 441	‹0.01	4,792 ± 562	ns
	ED_{90}	29,329 ± 4,661	7,272 ± 2,533	‹0.01	25,631 ± 963	ns

[1]ED_{50}, ED_{75} and ED_{90} were calculated using CompuSyn software as described in the Materials and Methods Section. Data represent the mean of three independent experiments ± SEM.
[2]Anti-OAcGD2 mAb 8B6 was combined with TMZ at the concentration of 40 µg/ml.
[3]p values indicate "TMZ alone" *vs.* "TMZ with 8B6".
[4]Isotype control antibody was combined with TMZ at the concentration of 40 µg/ml.
[5]p values indicate "TMZ alone" *vs.* "TMZ with IgG control" (ns, not significant).

Antibody 8B6 synergizes with TMZ *in vitro*

We next determined whether 8B6 would enhance TMZ cytotoxicity in GBM cells, using a MTT assay. In the three tested cell types we observe that TMZ alone induces a clear dose-dependent inhibition effect (Fig. 2a). The corresponding calculated ED_{50} values are 1,079 ± 146, 564 ± 77 µM and 1,313 ± 163 µM, for Hs683, GBM-15 and GBM-10 cells, respectively (Table 1). Addition of 8B6 strengthens the tumor cell viability inhibitory effect of TMZ in each cell type. The combination dose–response curves shifted towards sensitive side of the graph indicating that combination of 8B6 with TMZ is more efficient in inhibiting GBM cell viability (Fig. 2a). Moreover, the TMZ ED_{50} values are significantly lower in the presence of 8B6 ($p < 0.01$, Table 1). Similar results are found at ED_{75} and ED_{90} (Table 1).

To characterize the effect of the TMZ + 8B6 combination, we calculated the combination indices using the Chou–Talalay method.[25] We found that the CI values at ED_{50}, ED_{75} and ED_{90} are significantly <1 for each tested cell types ($p < 0.05$, Fig. 2b). This indicates a synergistic interaction (CI values: 0.51–0.72, Fig. 2b). We concluded that 8B6 is a possible adjuvant therapeutic agent to TMZ chemotherapy in GBM.

Based on our previous study, we went on investigating the possible involvement of an oncosis-like mechanism as a possible mode of action of 8B6 in the GBM cells sensitization to TMZ.[21] Oncosis is a programmed cell death associated with membrane damages and increased cell permeability, thereby allowing the uptake of cytotoxic therapeutic agents.[21] The analysis of the cell surface of GBM-10 cells after incubation with 8B6 under scan electron microscopy reveals that these cells display numerous pores in the presence of 8B6 (Fig. 2c). These membrane alterations induced by 8B6 correlate with a ~1.7 ± 0.2 intracellular TMZ concentration increase compared to the TMZ alone-treated cells, as determined by a mass-spectrometry quantification method (Fig. 2d). These results indicate the involvement of an oncosis-like mechanism in 8B6 GBM chemosensitization.

Antibody 8B6 increases TMZ-induced GBM cell death

To determine whether the increased drug permeability triggered by 8B6 would result in enhanced TMZ cytotoxicity, we assessed the amount of DNA breaks in GBM cells 72 hr post-treatment. Using FCM, we studied the expression of pH2AX, a widely used biomarker of cellular response to double-strand DNA breaks.[38] As shown in Figure 3a TMZ (50 µM) alone

Figure 2. Antibody 8B6 sensitizes glioblastoma (GBM) cells to temozolomide (TMZ). (a and b) Hs683, GBM-15 and GBM-10 cells were treated either singly or with combination of TMZ and 8B6, as indicated, and the MTT viability assay was carried out after 72 hr as described in the Materials and Methods Section. (a) Dose–response curves of the 8B6-, the TMZ- and the 8B6 + TMZ-treated cells, as indicated. Results are shown as mean ± SEM of three independent experiments run in triplicate. Untreated cells (gray). Results are shown as mean ± SEM of three independent experiments run in triplicate (*p ‹ 0.05; **p ‹ 0.01; ***p ‹ 0.001; ****p ‹ 0.0001; TMZ *vs.* TMZ + 8B6, Mann–Whitney test). (b) Combination index plots. The percentage survival values were transformed in Fraction affected (Fa) values and used to calculate combination index (measure of synergy, additivity and antagonism) using CompuSyn software, as described in the Materials and Methods section. Results are presented as mean ± SEM of three independent experiments, each run in triplicate. Data show that 8B6 has a synergistic effect with TMZ (CI ‹ 1; *p ‹ 0.05; unpaired Student's *t*-test). (c) Representative scanning electron micrograph of GBM-10 cells incubated for 30 min with 8B6 (40 µg/ml), isotype control antibody (40 µg/ml), TMZ (50 µM) or 8B6 + TMZ, as indicated. Membrane lesions are indicated with black arrows. Horizontal rods correspond to the scale bar (scale bar = 100 µm). (d) The membrane lesions induced by 8B6 seen in (c) correlate with an increased TMZ and TMZ metabolites intracellular uptake. After incubation, intracellular TMZ and metabolites were analyzed by mass spectrometry as described in the Materials and Methods section. Results are expressed as mean ± SEM of three independent experiments run in triplicate (***p ‹ 0.001; Mann–Whitney test). [Color figure can be viewed at wileyonlinelibrary.com]
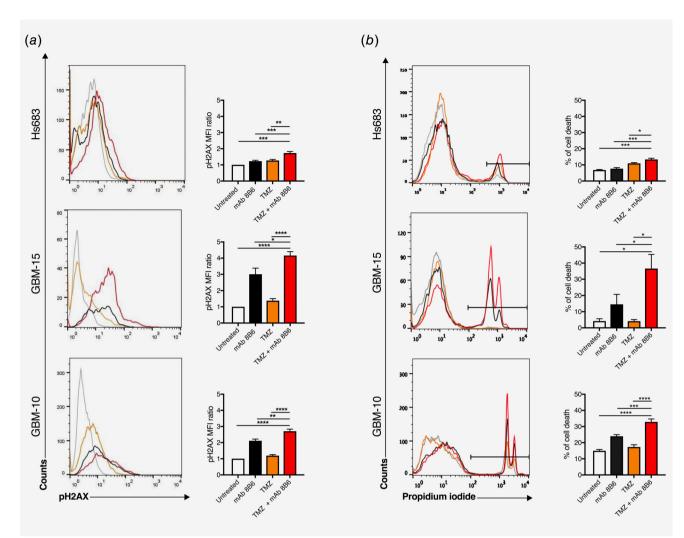
Figure 3. Antibody 8B6 increases temozolomide-induced DNA damage. (*a*) Left panels, representative histograms of pH2AX staining in the indicated GBM cells left untreated (gray) or treated for 72 hr with 8B6 (40 μg/ml, black), TMZ (50 μM, orange) or 8B6 + TMZ (red). Right panels, the geometric mean fluorescent intensities (MFIs) of the tumor cells in the left-hand side panels were normalized to the MFIs of untreated tumor cells. An increased intensity of pH2AX staining was seen in the cells incubated with 8B6 + TMZ, as indicated. Results are expressed as mean ± SEM of three individual experiments run in triplicate. (*b*) Combination of 8B6 with TMZ increases GBM cell death. Left panels, representative histograms of propidium iodide incorporation in the indicated GBM cells left untreated (gray) or treated 96 hr by either 8B6 (black), TMZ (orange) or 8B6 + TMZ (red). Right panels, mean percentage of dead cells ± SEM of three independent experiments, each run in triplicate. An increased percentage of death was seen in the cells incubated with 8B6 + TMZ, as indicated. Results are expressed as mean ± SEM of three individual experiments run in triplicate. *p ‹ 0.05; ***p ‹ 0.001; ****p ‹ 0.0001; Mann–Whitney test.

induces an ∼1.2 to 1.3 increase of the pH2AX MFI ratio in the three tested TMZ-resistant cell types (Fig. 3*a*). Differently, 8B6 (40 μg/ml) induces a ∼1.2-, ∼3- and ∼2.1-increase of the pH2AX MFI ratio in Hs683, GBM-15 and GBM-10 cells, respectively (Fig. 3*a*). More importantly, the MFI ratio analysis reveals that the amount of DNA breaks is significantly higher in the cells treated with the two-agent combination (Hs683: ∼1.7; GBM-15: ∼4.1; GBM-10: ∼2.7, Fig. 3*a*). The amount of DNA breaks correlates further with cell death induction detected by intracellular fluorescence of propidium iodide (Fig. 3*b*). Exposure to 50 μM TMZ for 72 hr induces the death of 10.9 ± 0.3, 4.1 ± 1.3 and 17.3 ± 0.1%, in Hs683, GBM-15 and GBM-10 cells, respectively (Fig. 3*b*). In the 8B6-treated

cells, the percentage of dead Hs683, GBM-15, and GBM-10 cells are 7.6 ± 0.6, 14.5 ± 1 and 23.9 ± 0.3%, respectively (Fig. 3*b*). Again, the strongest effect is seen in the cells treated with the combination regimen (Hs683: 13.5 ± 0.6%; GBM-15: 36.6 ± 1.8%; GBM-10: 32.8 ± 0.2%; Fig. 3*b*). Together, these data indicate that combination of 8B6 with TMZ is more effective in killing GBM cells than TMZ- and 8B6-monotherapy.

Antibody 8B6 combined with TMZ impairs GSC survival *in vitro*
The self-renewing GSCs constitute an important obstacle against effective therapy.[31,32] Thus, we assessed whether the
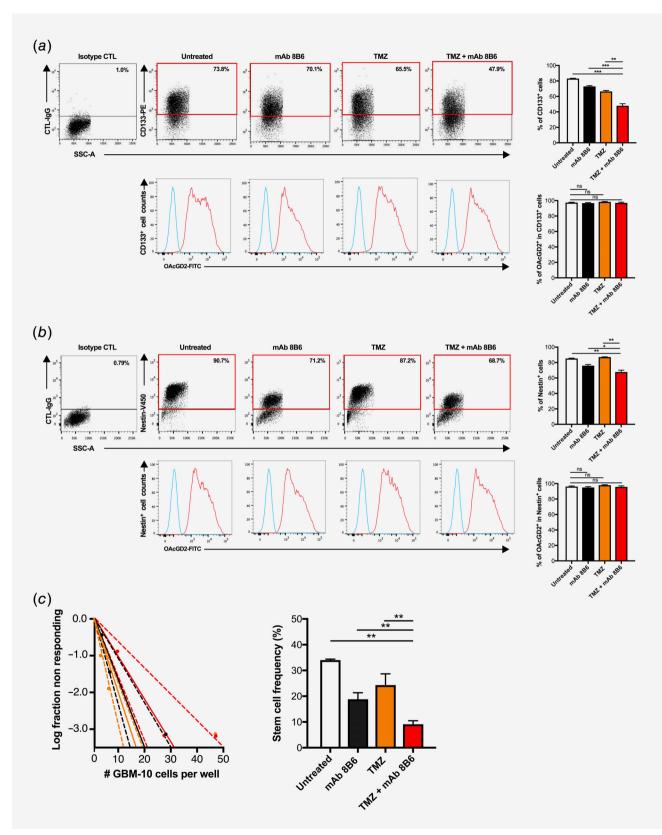
Figure 4. Legend on next page.

combination of anti-OAcGD2 8B6 to TMZ would impact the GSC subsets. We examined the frequency of Nestin⁺- and CD133⁺- cells in the GBM-10 after exposure to 8B6 (40 μg/ml) and TMZ (50 μM) used as single agents or in combination for 7 days. FCM analysis reveals that the combination regimen significantly reduces the Nestin⁺- and CD133⁺-cell frequencies (47.8 ± 2.7 and 67.6 ± 2.4%, respectively) compared to either 8B6- (72.9 ± 0.9 and 75.9 ± 1.5%, respectively) or TMZ-single agent alone treated cells (66.5 ± 1.29 and 87.0 ± 0.3%, respectively, Fig. 4b). To address a possible immune editing under 8B6 therapy, we subsequently evaluated OAcGD2 expression in the GSC⁺-subsets. Importantly, the MFI ratio analysis indicates that OAcGD2 expression remains unchanged in both the CD133⁺- and the Nestin⁺-GSC fractions after 8B6 exposure (Figs. 4a and 4b).

We further carried out a LDA to monitor the cell self-renewal capability.[27] Cells were incubated with TMZ (50 μM) and 8B6 (40 μg/ml) added alone or in combination, respectively, for 15 days. Thereafter, we scored each well for neurosphere formation and calculated the GSC frequency using ELDA software.[27] We found that the combination regimen significantly attenuates GBM-10 GSC self-renewal propensity. This is indicated by the decrease of the frequency of GBM-10 GSCs (9.1 ± 1.7%) compared to either 8B6- (18.8 ± 3.2%) or TMZ-monotherapy (24.3 ± 5.0%, Fig. 4c). We observed similar effects in the GBM-15 cells (Supporting Information Material S2). Collectively, these results suggest that 8B6 sensitizes GSCs to TMZ.

Antibody 8B6 combined with TMZ impairs GSC survival *in vivo*

To corroborate our *in vitro* findings, we evaluated the efficacy of the combination therapy *in vivo* using the GBM-10 cells. We selected these cells because they contain a fraction of GSCs (Fig. 1) and reproduce physical features of GBM *in vivo*.[39] Because of the limited injection volume that can be given intracerebrally in mice,[40] we established a subcutaneous model to evaluate the extension of the GSC pool after treatment. We started the treatments when tumors become palpable (30 mm³, Fig. 5a). We treated the mice with either TMZ (0.5 mg/kg i.p., Day 21, 24, 28 and 32), 8B6 (75 μg/mouse, Day 21, 24, 28 and 32) or in combination. We extrapolated the dose of TMZ between human (75 mg/m²) and mouse by following the recommendations established by Nair and Jacob.[41] We monitored the tumor volume and measured the body weight of these mice during the course of the experimentation. The event resulting in mouse euthanasia was disease progression, defined as the tumor volume exceeding 0.5 cm³. All therapies lead to tumor growth retardation compared to the control group treated with vehicle; the combination regimen however induces the strongest tumor growth inhibition (Fig. 5a). When we compare the tumor sizes between the monotherapy arms (TMZ: 265.2 ± 26.8 mm³, 8B6: 132.7 ± 27.1 mm³) and the combination group (26.8 ± 12.8 mm³), the differences are statistically significant ($p < 0.05$) on Day 46 (Fig. 5a). The mice do not show loss in weight, suggesting that the treatments are well tolerated (Fig. 5b).

We then collected the tumors of these mice to study the expression level of CD133, Nestin and OAcGD2 using FCM. Both CD133 and Nestin identify GSCs in GBM-10 xenografts (Fig. 5c). The analysis of the MFI ratio of CD133 expression reveals a clear decrease of the GSC pool in the combination therapy-group (2.78 ± 0.4), compared to other groups (PBS: 3.9 ± 0.6; 8B6: 4.4 ± 0.2; TMZ: 4.9 ± 1.2, Fig. 5c). Strikingly, TMZ-monotherapy increases the Nestin⁺-GSC pool (41.6 ± 22.1) compared to the control group (12.9 ± 3.3,

Figure 4. Antibody 8B6 combined with TMZ impairs the *in vitro* expansion of GBM stem-like cells (GSCs). (*a*) Cytofluorimetric analysis OAcGD2 expression in the CD133⁺-GBM-10 cells after 7 days exposition to TMZ (50 μM), 8B6 (40 μg/ml) or TMZ + 8B6. Upper left panels, representative dot-plot histograms showing the correlation of the expression CD133/SSC-A in the untreated-, the 8B6-, the TMZ- and the 8B6 + TMZ-treated cells, as indicated. The red quadrants indicate the CD133⁺-cell population. The histogram chart on the upper right shows the mean percentage of CD133⁺-cells ± SEM of three independent experiments, each run in triplicate. The combination regimen induces the strongest decrease of CD133⁺-GBM-10 cells. The cell treated in (*a*) were also subjected to OAcGD2 expression analysis. The lower left panels are representative histograms showing the expression level of OAcGD2 in the CD133⁺-cells. CD133⁺-GBM-10 cells were stained with isotype control antibody (blue) or 8B6 (red). The lower right histogram chart shows the mean percentage of OAcGD2⁺/CD133⁺-cells ± SEM of three independent experiments, each run in triplicate. The OAcGD2 expression level remains unchanged after treatments (ns, not significant; $p > 0.05$; Mann–Whitney test). (*b*) The same analysis was performed to study OAcGD2 expression in the Nestin⁺-GBM-10 cells. In the upper left panels, the representative dot-plot histograms show the correlation of the expression Nestin/SSC-A in the obtained after each regime treatments, as indicated. The red quadrants indicate the Nestin⁺-cell population. The histogram chart on the upper right shows the mean percentage of Nestin⁺-cells ± SEM of three independent experiments, each run in triplicate. The combination regimen induces the strongest decrease of Nestin⁺-GBM-10 cells. The lower left panels show representative histograms of OAcGD2 expression in the Nestin⁺-cells. Nestin⁺-GBM-10 cells were stained with isotype control antibody (blue) or 8B6 (red). The lower right histogram chart shows the mean percentage of OAcGD2⁺/Nestin⁺-cells ± SEM of three independent experiments, each run in triplicate. The OAcGD2 expression level remains unchanged after treatments. (*c*) GSC self-renewal capacity were assessed using a LDA, as described in the Materials and Methods section. The left dotted line plot shows a representative linear regression plot of limiting dilution assay for GBM-10 cells treated with 8B6 (40 μg/ml, black), TMZ (50 μM, orange) or TMZ + 8B6 (red) for 15 days. The change of slope of the trend line in the TMZ + 8B6 exposed cells suggests a differential tumorosphere formation ability. The dashed lines give the 95% confidence interval. The right histogram chart shows the GSCs frequency in response to vehicle (untreated), 8B6, TMZ or 8B6 + TMZ calculated with the ELDA software. The lowest GSCs frequency was observed with the combination therapy. Results are shown as mean ± SEM of three independent experiments, each run in triplicate. *$p < 0.05$; **$p < 0.01$; ***$p < 0.001$; Mann–Whitney test.
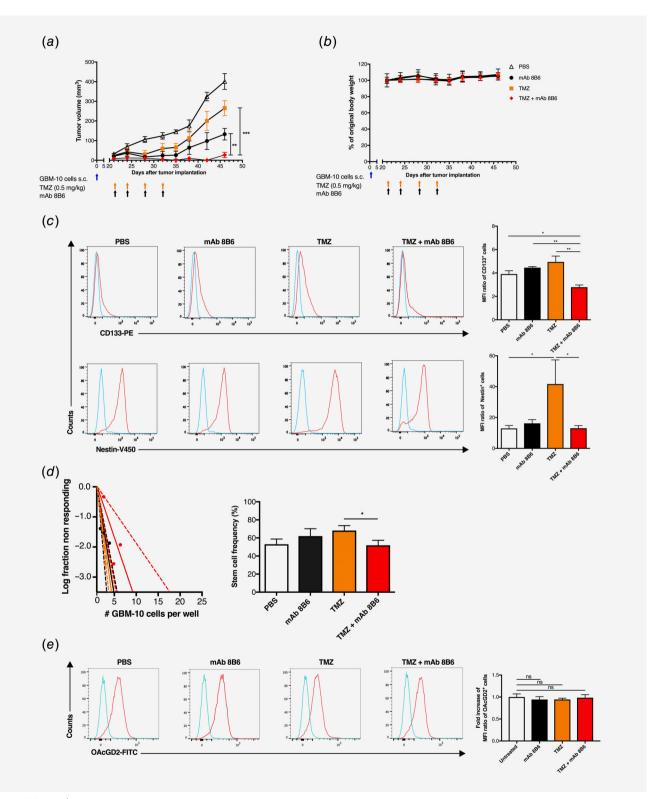
Figure 5. Legend on next page.

Fig. 5c). However, the combination therapy (13.0 ± 2.9) counteracts this effect (Fig. 5c). The LDA further reveals a significant GSC frequency decrease in tumors isolated from mice treated with the combination regimen (51.8 ± 5.5%) compared to the TMZ-treated group (68.1 ± 5.3%, Fig. 5d). Finally, we found that OAcGD2 expression level remained unchanged after 8B6 immunotherapy (Fig. 5e). These results are consistent with our *in vitro* findings. We conclude that anti-OAcGD2 adjuvant immunotherapy prevents the extension of GSCs induced by TMZ-monotherapy.

Discussion

An important prerequisite for improving the prognosis of patients with GBM is the elimination of the genotoxic-resistant subset of GSCs. In the present work, we characterize OAcGD2 ganglioside as a novel GBM stem-like cell marker that sensitizes chemoresistant GSCs to TMZ and overcome GBM recurrence driven by GSCs. The rationale for combining anti-OAcGD2 mAb with TMZ to improve the outcome of patients with GBM is suggested by earlier findings that anti-OAcGD2 mAbs induce death in GBM preclinical models.[20] Here, we first observe that the combination of 8B6 with TMZ results in decreased *in vitro* cell viability and increased tumor death in GBM cells compared to either 8B6- or TMZ-monotherapy. In addition, we demonstrate that 8B6 works synergistically with TMZ, having found that the CI values in all studied GBM cells were <1 independently of their TMZ-sensitivity. TMZ exposure does not influence the level of anti-OAcGD2 8B6 binding on these cells. Therefore, the underlying mechanism for this synergism cannot be attributed to the upregulation of OAcGD2 on the GBM cells. On the other hand, 8B6 induces an oncosis-like mechanism that leads to increased GBM cell TMZ uptake. This confirms and extends our previous findings in neuroblastoma models.[21] In addition, the higher level in DNA breaks seen in the GBM cells exposed to the combination therapy suggests a role of DNA damage signaling, regardless of the TMZ molecular resistance mechanisms. The specific mechanism by which the combination regimen acts on this signaling pathway remains however to be elucidated. Yet, another novel aspect of our investigation indicates that anti-OAcGD2 mAb can target GBM cells in order to avoid resistance to TMZ. This was particularly clear from the synergistic relationship seen in GBM cells with upregulated MGMT expression, a factor associated with TMZ treatment failure and GBM relapse.[28] Considering that almost half of GBMs are TMZ resistant primarily due to the expression of MGMT,[28] this finding provides a rationale to translate this combination regimen to patients with GBM.

An important consideration for effective control of GBM recurrence is to target GSCs in addition to eliminating the tumor bulk.[42] As mentioned earlier, currently known cell surface markers that are shared by the bulk tumor GBM cells and the GSC subset have demonstrated limited efficacy because they are susceptible to antigen escape.[18,19] There is thus a need for novel GSC antigens. As such, ganglioside GD2, the precursor of OAcGD2, represents a marker of GSCs[22] and its expression persists post immunotherapy.[43] However, given its tissue distribution pattern,[44] the O-acetyl derivative of GD2 provides a potential opportunity to develop safer immunotherapeutic strategies for patients with GBM.[20] To study the OAcGD2 expression in GSCs, we use GBM patient-derived cells containing GSCs.[20] We identify this cell subset in our models using CD133, Nestin or Sox2, three well-established stem cell markers.[33–35] Importantly, we find that OAcGD2 is expressed by both the GSC-positive subsets and the GSC-negative GBM cell fraction. This finding suggests that OAcGD2 represents a relevant antigen candidate for targeting these two cell compartments.

Figure 5. Therapeutic effect of temozolomide (TMZ) + 8B6 in the GBM-10 patient-derived glioblastoma (GBM) xenograft model. NOD/SCID mice bearing patient-derived GBM-10 subcutaneous xenograft were treated with vehicle (PBS, i.p.), TMZ alone (0.5 mg/kg, i.p.), 8B6 alone (150 μg, i.v.) or TMZ + 8B6, as indicated. Administration of PBS, 8B6 or TMZ treatment started on Day 21 after GBM-10 cells inoculation and was repeated three times on Day 24, 28 and 32. (*a*) Tumor growth was monitored and tumor volumes were calculated. Mean tumor volumes ± SEM of each treatment group (10 mice per group) are depicted, as indicated (**$p < 0.01$; ***< 0.001; Mann–Whitney test). (*b*) The mice weight was recorded for each treatment group, as indicated. Mean weight of mice on Day 21 was defined as 100% weight. Weight in each group remained stable for the period of treatment. Data are presented as the mean ± SEM of 10 mice/group. (*c*) Representative FCM histograms of GBM-10 cells harvested from the indicated treatment group, stained with either control antibody (blue) or the indicated stem cell marker antibody (red). The histogram chart on the right shows the geometric mean fluorescent intensities (MFIs) of the cells in (*c*) normalized to the MFIs of tumor cells stained with the control antibody, as indicated. TMZ + 8B6 therapy reduced the number of both CD133+- and Nestin+-cells compared to TMZ monotherapy. Data are presented as mean ± SEM of three individual mice, each run in triplicate. (*$p < 0.05$; **$p < 0.01$; Mann–Whitney test). (*d*) LDA were performed with cells harvested in (*a*) to determine the stem cell frequency in the tumor xenografts collected in each group of mice, as indicated. The left dotted line plot shows a representative linear regression plot of LDA for GBM-10 cells harvested from a 8B6- (black), TMZ- (orange) or TMZ + 8B6- (red) treated mouse. The change of slope of the trend line in the TMZ + 8B6 exposed cells suggests a differential tumorosphere formation ability. The dashed lines give the 95% confidence interval. The right histogram chart shows the GSCs frequency in GBM-10 cells harvested from the PBS-, 8B6-, TMZ- or 8B6 + TMZ-treated mice, as indicated. The GSC frequency values were calculated with the ELDA software. The lowest GSCs frequency was observed with the combination therapy (*$p < 0.05$; unpaired Student's *t*-test). (*e*) A FCM analysis was performed with the cells harvested from mice in (*a*) to assess the OAcGD2 expression in the different tumor samples, as indicated. The left panels show representative FCM histogram of GBM-10 cells harvested from the indicated treatment group, stained with either control antibody (blue) or 8B6 (red). The histogram chart on the right shows the mean fold increase of MFI ratio of the cells stained with 8B6 normalized to mean MFI ratio of the tumor cells stained with the control antibody, as indicated. The level of OAcGD2 expression remains stable after treatments (ns, not significant; $p > 0.5$).

GSCs constitute a highly tumorigenic self-renewal cell subset.[45] Consequently, after 8B6 treatment, we monitored the self-renewal capability of the GSCs in our GBM patient-derived cellular models using a neurosphere-formation limiting dilution assay.[27] Interestingly, we find that 8B6 compromises the self-renewal of glioblastoma stem-like cells *in vitro*. This finding once again confirms that anti-OAcGD2 mAbs can target the GSC-positive cell fraction in GBM tumors. More importantly, the combination of 8B6 with TMZ is more effective than the two agents alone. The synergistic action of the combination regimen is also reflected in the decreased expression of the CD133+- or the Nestin+-GBM cell populations, independently of their TMZ-sensitivity. Another novel aspect of our investigation, thus, suggests that the combination of 8B6 with TMZ impairs the ability of GSCs to drive tumor recurrence.

Antibody molecules do not cross the blood–brain barrier.[46] Even with malignant tumors where the blood–brain barrier is disrupted, tumor uptake is approximately 0.001%.[46] To bypass the blood–brain barrier antibody can be infused intracranially. The amount of mAb that can be delivered stereotaxically in mouse is limited.[40] We therefore tested the effect of combination regimen on the GSC subset using an ectopic model. In agreement with previous work,[47] TMZ-monotherapy expands the GSC subset in GBM-10 xenografts, evidenced by the increased expression of both CD133 and Nestin. This effect is also seen in their increased capacity to form neurospheres

in vitro. Importantly, the combination of 8B6 to TMZ significantly inhibits the tumor growth compared to TMZ used as a single agent. This combination induces the down-regulation of both CD133 and Nestin GSC expressions in GBM-10 xenografts, and further inhibits the capacity of GBM-10 cells isolated from tumors to expand as neuropsheres *in vitro*. Mostly, since a GSC-like phenotype could be accountable for TMZ-resistance and recurrence of the tumor, this combination likely performs through the control of stemness. Our data provide therefore a proof of concept that the combination regimen has significant antitumor effects. In patients, antibodies can be, infused locally into the resected tumor cavity to bypass the blood–brain barrier and achieve high tumor cell saturation.[48] Feasibility and efficacy of this technique will likely further increase with new emerging technologies.[49]

References

1. Delgado-Lopez PD, Corrales-Garcia EM. Survival in glioblastoma: a review on the impact of treatment modalities. *Clin Transl Oncol* 2016;18: 1062–71.
2. Stupp R, Mason WP, van den Bent MJ, et al. Radiotherapy plus concomitant and adjuvant temozolomide for glioblastoma. *N Engl J Med* 2005;352:987–96.
3. Ma W, Li N, An Y, et al. Effects of Temozolomide and radiotherapy on brain metastatic tumor: a systematic review and meta-analysis. *World Neurosurg* 2016;92:197–205.
4. Singh SK, Hawkins C, Clarke ID, et al. Identification of human brain tumour initiating cells. *Nature* 2004;432:396–401.
5. Lathia JD, Mack SC, Mulkearns-Hubert EE, et al. Cancer stem cells in glioblastoma. *Genes Dev* 2015;29:1203–17.
6. Kang MK, Kang SK. Tumorigenesis of chemotherapeutic drug-resistant cancer stem-like cells in brain glioma. *Stem Cells Dev* 2007;16: 837–47.
7. Pajonk F, Vlashi E, McBride WH. Radiation resistance of cancer stem cells: the 4 R's of radiobiology revisited. *Stem Cells* 2010;28:639–48.
8. Beier D, Schulz JB, Beier CP. Chemoresistance of glioblastoma cancer stem cells--much more complex than expected. *Mol Cancer* 2011;10:128.
9. Wang J, Wakeman TP, Lathia JD, et al. Notch promotes radioresistance of glioma stem cells. *Stem Cells* 2010;28:17–28.
10. Murphy SF, Varghese RT, Lamouille S, et al. Connexin 43 inhibition sensitizes Chemoresistant

Glioblastoma cells to Temozolomide. *Cancer Res* 2016;76:139–49.
11. Bhat KPL, Balasubramaniyan V, Vaillant B, et al. Mesenchymal differentiation mediated by NF-kappaB promotes radiation resistance in glioblastoma. *Cancer Cell* 2013;24:331–46.
12. Venur VA, Peereboom DM, Ahluwalia MS. Current medical treatment of glioblastoma. *Cancer Treat Res* 2015;163:103–15.
13. Reardon DA, Desjardins A, Vredenburgh JJ, et al. Phase 2 trial of erlotinib plus sirolimus in adults with recurrent glioblastoma. *J Neurooncol* 2010; 96:219–30.
14. Emlet DR, Gupta P, Holgado-Madruga M, et al. Targeting a glioblastoma cancer stem-cell population defined by EGF receptor variant III. *Cancer Res* 2014;74:1238–49.
15. Ahmed N, Salsman VS, Kew Y, et al. HER2-specific T cells target primary glioblastoma stem cells and induce regression of autologous experimental tumors. *Clin Cancer Res* 2010;16: 474–85.
16. Brown CE, Starr R, Aguilar B, et al. Stem-like tumor-initiating cells isolated from IL13Ralpha2 expressing gliomas are targeted and killed by IL13-zetakine-redirected T cells. *Clin Cancer Res* 2012;18:2199–209.
17. Hegde M, Corder A, Chow KK, et al. Combinational targeting offsets antigen escape and enhances effector functions of adoptively transferred T cells in glioblastoma. *Mol Ther* 2013;21:2087–101.
18. Hegde M, Mukherjee M, Grada Z, et al. Tandem CAR T cells targeting HER2 and IL13Ralpha2

mitigate tumor antigen escape. *J Clin Invest* 2016; 126:3036–52.
19. O'Rourke DM, Nasrallah MP, Desai A, et al. A single dose of peripherally infused EGFRvIII-directed CAR T cells mediates antigen loss and induces adaptive resistance in patients with recurrent glioblastoma. *Sci Transl Med* 2017;9: eaaa0984.
20. Fleurence J, Cochonneau D, Fougeray S, et al. Targeting and killing glioblastoma with monoclonal antibody to O-acetyl GD2 ganglioside. *Oncotarget* 2016;7:41172–85.
21. Faraj S, Bahri M, Fougeray S, et al. Neuroblastoma chemotherapy can be augmented by immunotargeting O-acetyl-GD2 tumor-associated ganglioside. *Oncoimmunology* 2017;7:e1373232.
22. Yeh SC, Wang PY, Lou YW, et al. Glycolipid GD3 and GD3 synthase are key drivers for glioblastoma stem cells and tumorigenicity. *Proc Natl Acad Sci USA* 2016;113:5592–7.
23. Oizel K, Chauvin C, Oliver L, et al. Efficient mitochondrial glutamine targeting prevails over Glioblastoma metabolic plasticity. *Clin Cancer Res* 2017;23:6292–304.
24. Denizot F, Lang R. Rapid colorimetric assay for cell growth and survival. Modifications to the tetrazolium dye procedure giving improved sensitivity and reliability. *J Immunol Methods* 1986;89: 271–7.
25. Chou TC, Talalay P. Quantitative analysis of dose-effect relationships: the combined effects of multiple drugs or enzyme inhibitors. *Adv Enzyme Regul* 1984;22:27–55.

Cancer Therapy and Prevention

26. Bahri M, Fleurence J, Faraj S, et al. Potentiation of anticancer antibody efficacy by antineoplastic drugs: detection of antibody-drug synergism using the combination index equation. *J Vis Exp* 2019;143:e58291.

27. Hu Y, Smyth GK. ELDA: extreme limiting dilution analysis for comparing depleted and enriched populations in stem cell and other assays. *J Immunol Methods* 2009;347:70–8.

28. Hegi ME, Diserens AC, Godard S, et al. Clinical trial substantiates the predictive value of O-6-methylguanine-DNA methyltransferase promoter methylation in glioblastoma patients treated with temozolomide. *Clin Cancer Res* 2004;10:1871–4.

29. Kokkinakis DM, Brickner AG, Kirkwood JM, et al. Mitotic arrest, apoptosis, and sensitization to chemotherapy of melanomas by methionine deprivation stress. *Mol Cancer Res* 2006;4:575–89.

30. Alvarez-Rueda N, Desselle A, Cochonneau D, et al. A monoclonal antibody to O-acetyl-GD2 ganglioside and not to GD2 shows potent antitumor activity without peripheral nervous system cross-reactivity. *PLoS One* 2011;6:e25220.

31. Parker NR, Khong P, Parkinson JF, et al. Molecular heterogeneity in glioblastoma: potential clinical implications. *Front Oncol* 2015;5:55.

32. Bastien JI, McNeill KA, Fine HA. Molecular characterizations of glioblastoma, targeted therapy, and clinical results to date. *Cancer* 2015;121:502–16.

33. Singh SK, Clarke ID, Terasaki M, et al. Identification of a cancer stem cell in human brain tumors. *Cancer Res* 2003;63:5821–8.

34. Gangemi RM, Griffero F, Marubbi D, et al. SOX2 silencing in glioblastoma tumor-initiating cells causes stop of proliferation and loss of tumorigenicity. *Stem Cells* 2009;27:40–8.

35. Wu B, Sun C, Feng F, et al. Do relevant markers of cancer stem cells CD133 and nestin indicate a poor prognosis in glioma patients? A systematic review and meta-analysis. *J Exp Clin Cancer Res* 2015;34:44.

36. Newlands ES, Stevens MF, Wedge SR, et al. Temozolomide: a review of its discovery, chemical properties, pre-clinical development and clinical trials. *Cancer Treat Rev* 1997;23:35–61.

37. Okada M, Ogino N, Matsumura M, et al. The process of subretinal strand formation. *Jpn J Ophthalmol* 1992;36:222–34.

38. Huang X, Halicka HD, Darzynkiewicz Z. Detection of histone H2AX phosphorylation on Ser-139 as an indicator of DNA damage (DNA double-strand breaks). *Curr Protoc Cytom* 2004;Chapter 7: Unit 7 27.

39. Jarry U, Chauvin C, Joalland N, et al. Stereotaxic administrations of allogeneic human Vgamma9Vdelta2 T cells efficiently control the development of human glioblastoma brain tumors. *Oncoimmunology* 2016;5: e1168554.

40. Liu C, Voth DW, Rodina P, et al. A comparative study of the pathogenesis of western equine and eastern equine encephalomyelitis viral infections in mice by intracerebral and subcutaneous inoculations. *J Infect Dis* 1970;122:53–63.

41. Nair AB, Jacob S. A simple practice guide for dose conversion between animals and human. *J Basic Clin Pharm* 2016;7:27–31.

42. Reya T, Morrison SJ, Clarke MF, et al. Stem cells, cancer, and cancer stem cells. *Nature* 2001;414: 105–11.

43. Kramer K, Gerald WL, Kushner BH, et al. Disialoganglioside G(D2) loss following monoclonal antibody therapy is rare in neuroblastoma. *Clin Cancer Res* 1998;4:2135–9.

44. Yuki N, Yamada M, Tagawa Y, et al. Pathogenesis of the neurotoxicity caused by anti-GD2 antibody therapy. *J Neurol Sci* 1997;149:127–30.

45. Denysenko T, Gennero L, Roos MA, et al. Glioblastoma cancer stem cells: heterogeneity, microenvironment and related therapeutic strategies. *Cell Biochem Funct* 2010;28:343–51.

46. Kemshead JT, Jones DH, Lashford L, et al. 131-I coupled to monoclonal antibodies as therapeutic agents for neuroectodermally derived tumors: fact or fiction? *Cancer Drug Deliv* 1986;3:25–43.

47. Auffinger B, Tobias AL, Han Y, et al. Conversion of differentiated cancer cells into cancer stem-like cells in a glioblastoma model after primary chemotherapy. *Cell Death Differ* 2014;21: 1119–31.

48. Wersall P, Ohlsson I, Biberfeld P, et al. Intratumoral infusion of the monoclonal antibody, mAb 425, against the epidermal-growth-factor receptor in patients with advanced malignant glioma. *Cancer Immunol Immunother* 1997;44:157–64.

49. Bousquet G, Darrouzain F, de Bazelaire C, et al. Intrathecal Trastuzumab halts progression of CNS metastases in breast cancer. *J Clin Oncol* 2016;34: e151–5.

Cancer Therapy and Prevention

6:43 PM DEC 01, 2022

THE MOMENT YOUR GUT INSTINCT
WAS BACKED BY SCIENTIFIC
RESULTS_

THE DIFFERENCE OF
BREAKTHROUGH MOMENTS

WITH COMPLETE SOLUTIONS FOR GROUNDBREAKING DISCOVERIES FROM A TRUSTED PARTNER.

Your next breakthrough could be closer than you imagine, especially with the right resources to help you advance your research. At BD, we are dedicated to helping you get the data you need, when, where and how you need it. Our integrated solutions in instrumentation, software and reagents are optimized to work together to bring you closer to your next breakthrough moment. And you can depend on us for world-class training, service and support to help you get the most from the results your research depends on. Discover a range of optimized solutions that open endless possibilities for your future research. **Discover the new BD.**

Learn how you can advance your research >

BD